N.A.E.

R. & M. No. 2738
(13,155)
A.R.C. Technical Report

MINISTRY OF SUPPLY

AERONAUTICAL RESEARCH COUNCIL
REPORTS AND MEMORANDA

Tests on a Swept-back Wing and Body in the Compressed Air Tunnel

By

C. SALTER, M.A., C. J. W. MILES and Miss H. M. LEE, B.Sc.
of the Aerodynamics Division, N.P.L.

LONDON: HER MAJESTY'S STATIONERY OFFICE
1953
FIVE SHILLINGS NET

Tests on a Swept-back Wing and Body in the Compressed Air Tunnel

By

C. SALTER, M.A., C. J. W. MILES AND MISS H. M. LEE, B.Sc.,

of the Aerodynamics Division, N.P.L.

*Reports and Memoranda No. 2738**
May, 1950

Summary.—The model consisted of a swept-back wing of symmetrical section and a long cylindrical body. The aspect ratio was 3·29, the taper ratio 2·75, the sweep of the quarter-chord line 42·5 deg, the maximum thickness/chord ratio at the root 8·6 per cent and at the tip 10 per cent.

It has been tested over a range of Reynolds numbers of $0 \cdot 5 \times 10^6$ to 13×10^6 and results are given of lift, drag and pitching moment for angles of incidence up to 30 deg.

Scale effect is not large and at the higher values of R, $C_{L\,max}$ is slightly less than unity while $C_{D\,min}$ is about 0·010. In the same range of R, $dC_L/d\alpha$ ($C_L \rightarrow 0$, α in degrees) is 0·056 to 0·057, but this slope is not maintained at the higher values of C_L.

The slope of the C_D vs. $C_L{}^2$ curve decreases with R to a value of 0·105. For the aspect ratio of this wing, 3·29, $1/\pi A = 0 \cdot 097$, a sharp increase in nose-down moment occurs at an incidence of roughly one degree less than the value at which the C_L vs. α curve flattens out.

Observations, both visual and photographic, have been made with tufted upper surface and the critical change in the value of dC_m/dC_L is found to be consistently related to an instantaneous alteration of the flow picture.

All changes of the flow pattern commence at the outboard parts of the trailing edge and at the tips and move inwards. Severe loss of lift corresponds to violent stall spreading inwards from the tips.

A selection of flow pictures is reproduced.

Model.—A plan view of the model is given in Fig. 1 and the main dimensions are given in Table 1.

The swept-back metal wing was made in two parts bolted together at the centre and was situated in a 'mid-wing' position in a cylindrical body. It was constructed with a negative dihedral (− 1 deg) and was set at + $1\frac{1}{2}$ deg incidence to the body axis.

The section was symmetrical and is illustrated for datum root chord and tip chord in Fig. 2. Ordinates are given in Table 2.

The body, made of wood and Phenoglazed, was rounded at the nose and stub-ended at the tail, no tail unit being provided. Neither was any body wing fillet incorporated while the trailing edge extended in straight lines right up to the fuselage.

*Published with the permission of the Director, National Physical Laboratory.

(23118) A

Range of Investigation.—The tests covered the range of Reynolds numbers from $0 \cdot 5 \times 10^6$ to 13×10^6 at angles of incidence of the datum root chord varying from $-2\frac{1}{2}$ deg to $+30$ deg, and measurements were made of lift, drag and pitching moment.

The rear half of the upper surface of the wing was afterwards tufted in order to examine the changes of flow pattern. These were studied visually for all values of R and of α, and photographs were taken of typical flow conditions at $R = 8 \times 10^6$ approximately. The flow on the under surface was also examined with a tufted probe at atmospheric pressure and low Reynolds number.

Tables and Figures.—Tables are appended containing the results of the investigations. A further run was also made at high pressure and low wind speed ($R = 4 \cdot 9 \times 10^6$) for comparison with $R = 4 \cdot 85 \times 10^6$ taken at low pressure and high wind speed. Agreement was almost exact.

Typical curves of C_L against α and of C_m and C_D against C_L are drawn in Figs. 3 and 4 for a moderate, a medium and a high Reynolds number, namely $4 \cdot 85 \times 10^6$, $7 \cdot 02 \times 10^6$ and $12 \cdot 9 \times 10^6$ respectively. Curves showing the variation of $C_{L\,max}$, $dC_L/d\alpha$ ($C_L \rightarrow 0$), and $C_{D\,min}$ with R are included in the same figures. That part of the drag which is proportional to C_L^2 is also illustrated in Fig. 4.

Zero incidence refers to the attitude of the machine when the datum root chord is horizontal. Values of C_m are given about a line perpendicular to the body axis and passing through the datum root chords at a distance of $1 \cdot 14$ ft from the theoretical apex of the leading edge, *i.e.*, the point of intersection of the two halves of the leading edge continued into the body.

Fig. 3 also includes a curve showing the relation between a critical change in the flow pattern and a critical region with respect to the values of $dC_L/d\alpha$.

Results.—The value of $C_{L\,max}$ rises from $0 \cdot 92$ (below $R = 1 \cdot 5 \times 10^6$) to rather less than unity above $R = 4 \times 10^6$ with a very slight falling off at the top of the range (Fig. 3).

The slope of the lift curve at low values of C_L varies in a somewhat similar manner (Fig. 3), but, except at low values of R, the slope decreases appreciably at a point which is not well defined but where, on the average, the value of C_L is about one third of the maximum (Table 4). The angle of incidence at zero lift is very close to $0 \cdot 4$ deg throughout.

Fig. 4 includes typical curves of C_m against C_L. It will be observed that at an angle of incidence somewhat less than the stalling angle, C_m decreases sharply to a minimum, corresponding to a rapid increase in nose-down pitching moment, but recovery follows fairly quickly.

Consideration of Fig. 3 and Table 5 will show that the minimum in the C_m curve corresponds to the point at which the C_L vs. α curve begins to flatten out and it will be demonstrated later that the sharp increase in the absolute value of dC_m/dC_L, which occurs about one degree earlier, appears to be associated with a very sudden change in the flow pattern.

Typical curves of C_D vs. C_L are plotted in Fig. 4 and the variation of $C_{D\,min}$ is also given (*see also* Table 4). $C_{D\,min}$ at the higher Reynolds numbers is rather less than $0 \cdot 010$, and minimum drag throughout occurs at average values of $\alpha = 0 \cdot 7$ deg and $C_L = 0 \cdot 01$ to $0 \cdot 02$.

In those cases where sufficient observations have been taken to enable the slope of the C_D vs. C_L^2 curve to be measured at low values of C_L the results are recorded in Table 4 and plotted in Fig. 4. It falls with increasing Reynolds number to a value of $0 \cdot 105$ at $R = 13 \times 10^6$. The aspect ratio of the wing being $3 \cdot 29$, $1/\pi A = 0 \cdot 097$.

In Ref. 1 a somewhat similar variation is shown for a wing of aspect ratio $3 \cdot 07$, leading-edge sweep back $50 \cdot 2$ deg, and taper ratio 4. For this particular wing the value at $R = 10 \times 10^6$ was found to be about $0 \cdot 11$ ($1/\pi A = 0 \cdot 104$).

All values of C_D include a correction in respect of the horizontal buoyancy effect due to static pressure gradient in the tunnel. The magnitude of the correction is $+ 0\cdot0015$ which has been added to the observed values.

Visual and Photographic Technique.—A method has been devised of viewing tufts on the upper surface of the model, after reflection in a mirror, through one of the small spy holes in the shell of the Compressed Air Tunnel. Illumination is obtained from a bank of car headlamp bulbs which are strong enough to withstand the maximum pressure of 25 atmospheres. Araldite adhesive number 101 with Hardener 951 is used for fixing the tufts to the metal surface.

An F.24 camera is also set up in such a position as to enable photographs to be taken at all angles of incidence. In this case illumination can be continuous for a few seconds using the headlamp bulbs, or intermittent using a flash discharge tube and power pack. Provided the amount of movement of the tufts is not excessive the first method is entirely satisfactory (and more convenient) and shows not only the mean direction but also the amount of roughness in the local flow. The intermittent method permits single exposures of very small duration or superimposed exposures (say ten or so). This method results in better pictures where the movement of the tufts is very violent as in the stalled region.

In all cases the greatest difficulty is that of obtaining a clear background especially with doubly curved surfaces and methods of producing a dull finish (without disturbing the profile) have so far been less effective than the practice of polishing the wing and suitably locating the source of light.

Polaroid filters are known to be very effective in respect of non-metallic surfaces and in fact the use of two such filters, one in the incident and one in the reflected beam, has been found to result in a considerable improvement in the relative intensity of tuft and background in respect of this metal wing. The loss of illumination is at present however a severe handicap but the method is being investigated further.

Tuft Photographs.—Typical photographs covering a range of incidence of 6 deg to 25 deg at $R = 8 \times 10^6$ approximately are reproduced in Figs. 5 and 6. For clarity some of these have been touched up slightly, and because of the pronounced distortion due to perspective, lines have been drawn to indicate true direction parallel to the body axis.

The lettered and numbered photograph (Fig. 5a) is inserted to assist in the discussion of the flow picture.

Sequence of Changes of Flow Pattern.—The flow has been studied visually at all values of Reynolds number and for $R =$ about 8×10^6 the changes are as follows:—

At small angles of incidence a slight inflow develops in the region A1, A2, B2 of the first two rows of tufts (Figs. 5a and 5b) and a slight outflow in the middle part of the third row. This pattern develops gradually until at 11 deg the inflow is more pronounced and outflow occurs all along the trailing edge, increasing in strength from the body outwards and also affecting the tufts near the body in the second row (Fig. 5c).

By 17 deg all inflow disappears again and outflow exists everywhere except in the centre of row A and is very strong along row C again increasing towards the tip (Fig. 6a), some of the tufts are now showing signs of unsteadiness.

So far, except for sudden and not very consistent increases in deflection at B1 and C1, the variations have been progressive. At 18 deg however a change takes place when the tufts on the outer half of the wing very suddenly swing out at about 90 deg (some more, some less) to the body axis and become very unsteady. At the same time outflow on the inner half increases somewhat (*cf.* Figs. 6a and 6b).

At higher angles the outflow and unsteadiness and the strong reverse flow developing at the tip spread gradually inwards, but not until 29 deg does the violent movement of the tufts extend to the body-wing junction.

Using a tufted probe the flow on the under surface has also been examined but only at atmospheric pressure ($R = 0{\cdot}6 \times 10^6$). Except for the usual spilling over at the tip the flow remains everywhere parallel to the body axis up to an incidence of about 16 deg. Beyond this, outflow begins to build up around a point about one quarter of the tip chord from the leading edge and the same distance inwards from the tip. This gradually extends inwards parallel to the leading edge but only slightly rearwards becoming much intensified so that at 29 deg the direction of flow is parallel to the leading edge. On the rear two-thirds of the under surface however the tufts remain steadily parallel to the body axis.

Comments on Tuft Experiments.—Except for some differences in the value of α these variations of flow pattern on the upper surface apply to all Reynolds numbers above about 3×10^6. At low values of R there are no sudden transformations but the overall development, although less well-defined, is much the same.

In Fig. 3 points are plotted against R showing the incidence of

(a) the sudden decrease in the value of C_m,

(b) the instantaneous swing of the outboard tufts,

(c) the minimum value of C_m (about the specified axis),

(d) the points where the C_L vs. α curve begins to flatten out.

It appears that the rapid decrease in pitching moment coincides with the instantaneous change in the flow pattern, and the loss of lift with the minimum in the C_m-curve and with the violent reverse flow developing at the tip. The former effect occurs at an angle of incidence of the order of 1 deg before the latter.

It is rather difficult to speak of a stagnation point with this type of wing but what may be called the stagnation region as well as the stall, proceeds inwards from the tip. The gradual change appears to be inevitable but a modification of the outer part of the wing might be devised to improve the aerodynamic characteristics of the machine by delaying the sudden breakdown of flow.

REFERENCES

No.	*Author(s)*	*Title, etc.*
1	R. Jones, C. J. W. Miles and P. S. Pusey	Experiments in the Compressed Air Tunnel on Swept-back Wings including two Delta Wings. A.R.C. 11,354. March, 1948.
2	B. Thwaites	On the Design of Aerofoil Sections for High-Speed Aircraft. A.R.C. 9076. October, 1945.

TABLE 1

Main Dimensions of Model

Span	3·725 ft
Gross wing area (L.E. and T.E. joined straight across fuselage)	4·22 sq ft
Nett Wing area	3·50 sq ft
Gross mean chord $= b/a$	1·1325 ft
Aspect Ratio $= a/d$	3·29
Taper Ratio	2·75
Sweep of quarter-chord line	42·5 deg
,, ,, leading edge	46·7 deg
,, ,, trailing edge	25·9 deg
Geometric twist	nil
Dihedral (datum root chord horizontal)	−1·0 deg
Theoretical centre-line chord	1·728 ft
Chord at extreme tip (L.E. and T.E. produced)	0·611 ft
Datum root chord (0·347 ft from centre-line)	1·481 ft
,, ,, ,, Maximum t/c	8·6 per cent
Tip chord Maximum t/c	10·0 per cent
Wing setting to fuselage centre-line	1·5 deg
Overall length of fuselage	4·58 ft
Maximum diameter fuselage	0·47 ft
Distance from nose to theoretical apex of L.E.	0·957 ft
,, ,, theoretical apex of L.E. to moments axis	1·14 ft
,, ,, moments axis to plane of datum root chords	nil

TABLE 2

Wing Section Ordinates

Datum Root Chord		Tip Chord (L.E. and T.E. produced)	
Distance from L.E. (inches)	Half Width (inches)	Distance from L.E. (inches)	Half Width (inches)
0	0·0	0	0·0
0·089	0·15	0·037	0·072
0·222	0·22	0·092	0·105
0·444	0·294	0·183	0·141
0·889	0·394	0·367	0·189
1·333	0·465	0·55	0·223
1·778	0·521	0·733	0·25
2·667	0·605	1·10	0·29
3·555	0·668	1·467	0·32
4·444	0·713	1·833	0·342
5·333	0·742	2·20	0·355
6·222	0·76	2·567	0·364
7·111	0·765	2·933	0·367
8·00	0·76	3·30	0·364
8·889	0·742	3·667	0·355
10·667	0·662	4·40	0·317
12·444	0·537	5·133	0·257
14·222	0·37	5·867	0·177
17·778 (T.E.)	0·007	7·333 (T.E.)	0·007
Max. t/c = 8·6 per cent at $0·4c$		Max. t/c = 10 per cent at $0·4c$	
L.E. Radius = 0·16 inches		L.E. Radius = 0·077 inches	

The section was designed by the Thwaites method (A.R.C. 9076)[2]. The approximate velocity distribution at zero lift was assumed to be constant to $0·35c$ and over the nose region the section resembled HSA1 (t/c = 10 per cent), the leading-edge radius being proportional to the thickness of the section. The trailing edge was brought up to a finite thickness by straight-line fairings on the theoretical profile.

TABLE 3

$P = 1\cdot0$ Atmos. $V = 70\cdot9$ F.P.S.		$\rho V^2 = 12\cdot08$ lb/sq ft $R = 0\cdot515 \times 10^6$		$P = 4\cdot45$ Atmos. $V = 57\cdot3$ F.P.S.		$\rho V^2 = 34\cdot1$ lb/sq ft $R = 1\cdot76 \times 10^6$		$P = 9\cdot11$ Atmos. $V = 60\cdot4$ F.P.S.		$\rho V^2 = 76\cdot9$ lb/sq ft $R = 3\cdot84 \times 10^6$	
α	C_L	C_D	C_m	α	C_L	C_D	C_m	α	C_L	C_D	C_m
− 2·35	−0·147	0·0158	−0·0073	− 2·4	−0·157	0·0140	−0·0072	− 2·4	−0·158	0·0140	−0·0052
− 1·1	−0·081	0·0134	−0·0068	− 1·15	−0·091	0·0108	−0·0068	− 0·15	−0·089	0·0108	−0·0074
+ 0·1	−0·016	0·0118	−0·0063	+ 0·1	−0·024	0·0099	−0·0070	+ 0·05	−0·019	0·0092	−0·0079
1·35	+0·050	0·0115	−0·0057	1·3	+0·043	0·0099	−0·0074	1·3	+0·048	0·0095	−0·0082
2·6	0·114	0·0131	−0·0049	2·55	0·106	0·0111	−0·0060	2·55	0·112	0·0113	−0·0080
3·8	0·175	0·0151	−0·0037	3·75	0·173	0·0134	−0·0066	3·75	0·181	0·0137	−0·0098
6·25	0·320	0·0251	−0·0103	6·2	0·306	0·0214	−0·0104	6·2	0·316	0·0212	−0·0132
8·7	0·470	0·0487	−0·0234	8·7	0·438	0·0328	−0·0136	8·65	0·451	0·0329	−0·0167
9·9	0·540	0·0674	−0·0243	11·15	0·568	0·514	−0·0149	11·15	0·582	0·0483	−0·0199
11·15	0·606	0·0892	−0·0221	13·55	0·716	0·103	−0·0325	13·55	0·710	0·0680	−0·0236
12·4	0·662	0·109	−0·0174	14·8	0·768	0·137	−0·0308	16·0	0·836	0·0923	−0·0278
13·6	0·710	0·135	−0·0135	16·0	0·822	0·171	−0·0260	18·45	0·920	0·183	−0·0327
14·85	0·758	0·161	−0·0122	17·3	0·832	0·213	−0·0164	21·0	0·976	0·296	−0·0331
16·1	0·794	0·191	−0·0093	18·5	0·879	0·248	−0·0154	22·35	0·974	0·330	−0·0330
17·35	0·836	0·217	−0·0089	19·8	0·902	0·282	−0·0149	23·65	0·976	0·376	−0·0314
18·55	0·868	0·254	−0·0085	21·05	0·916	0·319	−0·0150	25·0	0·976	0·414	−0·0314
19·85	0·884	0·284	−0·0073	22·4	0·929	0·367	−0·0152	26·35	0·982	0·448	−0·0312
21·15	0·906	0·319	−0·0080	23·7	0·930	0·390	−0·0162	27·7	0·964	0·479	−0·0339
22·5	0·914	0·349	−0·0093	25·05	0·935	0·416	−0·0202	29·1	0·945	0·498	−0·0453
23·75	0·919	0·381	−0·0154	26·45	0·906	0·442	−0·0278				
25·15	0·912	0·418	−0·0249	27·8	0·894	0·464	−0·0376				
27·5	0·898	0·451	−0·0340	29·15	0·895	0·489	−0·0474				

TABLE 3—*continued*

$P = 9 \cdot 78$ Atmos. $V = 73 \cdot 2$ F.P.S.		$\rho V^2 = 120$ lb/sq ft $R = 4 \cdot 85 \times 10^6$		$P = 13 \cdot 1$ Atmos. $V = 60 \cdot 9$ F.P.S.		$\rho V^2 = 111$ lb/sq ft $R = 5 \cdot 38 \times 10^6$		$P = 16 \cdot 6$ Atmos. $V = 56 \cdot 2$ F.P.S.		$\rho V^2 = 117$ lb/sq ft $R = 6 \cdot 08 \times 10^6$	
α	C_L	C_D	C_m	α	C_L	C_D	C_m	α	C_L	C_D	C_m
− 2·4	−0·162	0·0140	−0·0041	− 2·4	−0·160	0·0141	−0·0039	− 2·4	−0·162	0·0040	−0·0041
+ 2·55	+0·113	0·0103	−0·0080	− 1·15	−0·090	0·0116	−0·0054	− 1·15	−0·093	0·0116	−0·0051
7·45	0·386	0·0255	−0·0159	+ 0·05	−0·020	0·0097	−0·0071	+ 0·05	−0·022	0·0098	−0·0067
12·35	0·651	0·0566	−0·0235	1·3	+0·048	0·0100	−0·0076	1·3	+0·047	0·0098	−0·0079
17·25	0·897	0·103	−0·0312	2·55	0·117	0·0116	−0·0085	2·55	0·116	0·0112	−0·0087
18·45	0·967	0·121	−0·0402	3·75	0·184	0·0140	−0·0105	3·75	0·185	0·0139	−0·0109
19·7	0·894	0·219	−0·0462	6·2	0·323	0·0211	−0·0142	6·2	0·321	0·0214	−0·0151
21·0	0·989	0·275	−0·0426	8·65	0·461	0·0331	−0·0185	8·65	0·452	0·0321	−0·0192
22·35	0·993	0·324	−0·0408	11·1	0·586	0·0527	−0·0214	11·15	0·585	0·0480	−0·0234
23·65	0·986	0·370	−0·0414	13·55	0·707	0·0691	−0·0251	13·55	0·706	0·0674	−0·0269
25·0	0·980	0·410	−0·0450	16·0	0·838	0·0894	−0·0295	16·0	0·830	0·0906	−0·0308
26·35	0·980	0·438	−0·0387	18·4	0·964	0·121	−0·0347	18·45	0·946	0·120	−0·0337
27·75	0·952	0·465	−0·0387	19·7	0·991	0·162	−0·0467	19·7	0·992	0·181	−0·0500
29·1	0·933	0·495	−0·0477	21·0	0·992	0·274	−0·0389	21·0	0·975	0·270	−0·0401
				22·35	0·988	0·322	−0·0357	22·35	0·989	0·320	−0·0395
				23·65	0·987	0·360	−0·0371	23·65	0·984	0·360	−0·0373
				25·0	0·985	0·402	−0·0388	25·0	0·991	0·404	−0·0401
				26·35	0·988	0·431	−0·0372	26·35	0·985	0·443	−0·0383
				27·7	0·988	0·460	−0·0417	27·7	0·976	0·474	−0·0474
				29·1	0·940	0·483	−0·0485	29·1	0·931	0·491	−0·0524

TABLE 3—*continued*

P =19·0 Atmos. V =56·8 F.P.S.	ρV^2=137 lb/sq ft R =7·02 × 10^6			P =16·8 Atmos. V =75·4 F.P.S.	ρV^2=214 lb/sq ft R =8·3 × 10^6			P =17·9 Atmos. V =72·2 F.P.S.	ρV^2=217 lb/sq ft R =8·8 × 10^6		
α	C_L	C_D	C_m	α	C_L	C_D	C_m	α	C_L	C_D	C_m
− 2·4	−0·159	0·0141	−0·0037	− 2·45	−0·162	0·0138	−0·0034	− 2·45	−0·158	−0·0139	−0·0040
− 1·15	−0·094	0·0116	−0·0046	+ 3·75	+0·184	0·0133	−0·0109	− 1·2	−0·090	0·0116	−0·0051
+ 0·05	−0·013	0·0100	−0·0066	11·1	0·593	0·0474	−0·0243	+ 0·1	−0·027	0·0102	−0·0061
1·3	+0·049	0·0100	−0·0076	17·25	0·907	0·104	−0·0337	1·3	+0·049	0·0101	−0·0078
2·55	0·116	0·0112	−0·0085	18·4	0·953	0·151	−0·0405	2·55	0·118	0·0113	−0·0090
3·75	0·192	0·0141	−0·0111	19·65	0·968	0·234	−0·0435	3·75	0·183	0·0133	−0·0110
6·2	0·324	0·0215	−0·0145	21·0	0·972	0·283	−0·0347	6·2	0·318	0·0208	−0·0150
8·65	0·457	0·0329	−0·0189	23·35	0·983	0·331	−0·0342	8·65	0·450	0·0231	−0·0193
11·1	0·588	0·0477	−0·0231	23·65	0·980	0·370	−0·0357	11·15	0·581	0·0477	−0·0242
13·55	0·712	0·0673	−0·0274	25·0	0·972	0·415	−0·0355	13·55	0·708	0·0675	−0·0287
16·0	0·844	0·0893	−0·0316	26·35	0·970	0·445	−0·0357	16·0	0·828	0·0907	−0·0321
18·45	0·968	0·124	−0·0357	27·65	0·958	0·464	−0·0460	18·45	0·941	0·147	−0·0408
19·7	0·994	0·179	−0·0418	29·05	0·925	0·487	−0·0540	19·75	0·953	0·233	−0·0429
21·05	0·978	0·277	−0·0352					21·1	0·958	0·282	−0·0354
22·35	0·994	0·325	−0·0356					22·4	0·965	0·326	−0·0344
23·7	0·978	0·374	−0·0348					23·75	0·956	0·364	−0·0338
25·05	0·998	0·411	−0·0334					25·05	0·968	0·408	−0·0354
26·4	0·982	0·445	−0·0334					26·45	0·942	0·445	−0·0377
27·75	0·958	0·468	−0·0420					27·75	0·940	0·458	−0·0436
29·1	0·924	0·485	−0·0484					29·15	0·917	0·484	−0·0543

TABLE 3—*continued*

P =22·6 Atmos. ρV^2=260 lb/sq ft
V =71·9 F.P.S. R =10·5 × 10^6

α	C_L	C_D	C_m
− 2·45	−0·162	0·0139	−0·0029
+ 2·55	+0·116	0·0108	−0·0083
7·45	0·388	0·0258	−0·0173
12·35	0·658	0·0563	−0·0274
16·05	0·839	0·0915	−0·0325
17·25	0·904	0·116	−0·0381
18·45	0·950	0·184	−0·0490
19·8	0·954	0·244	−0·0351
21·1	0·959	0·294	−0·0305
22·4	0·961	0·334	−0·0298
23·7	0·971	0·378	−0·0325
25·05	0·969	0·414	−0·0341
26·4	0·979	0·444	−0·0392
27·75	0·933	0·467	−0·0462

P =23·4 Atmos. ρV^2=352 lb/sq ft
V =82·3 F.P.S. R =12·9 × 10^6

α	C_L	C_D	C_m
− 2·45	−0·158	0·0138	−0·0037
− 1·2	−0·089	0·0113	−0·0054
0	−0·020	0·0099	−0·0065
1·25	+0·050	0·0099	−0·0073
2·55	0·119	0·0113	−0·0092
3·75	0·189	0·0135	−0·0113
6·2	0·328	0·0206	−0·0153
8·7	0·460	0·0317	−0·0197
11·15	0·592	0·0480	−0·0248
13·55	0·723	0·0678	−0·0292
16·05	0·840	0·0929	−0·0313
17·2	0·906	0·144	−0·0492
18·45	0·929	0·214	−0·0367
19·8	0·938	0·265	−0·0282
21·15	0·949	0·310	−0·0269
22·45	0·955	0·345	−0·0295
23·7	0·970	0·385	−0·0314
25·05	0·967	0·421	−0·0318
26·45	0·940	0·440	−0·0361
27·8	0·909	0·463	−0·0437

TABLE 4

$\frac{R}{10^6}$	$C_{L\,\max}$	$C_{D\,\min}$	$dC_L/d\alpha$ (α in degrees)		Slope of curves of C_D vs. $C_L{}^2$
			$C_L \to 0$	$C_L \to$ stall	
0·515	0·920	0·0113	0·053	—	—
1·76	0·930	0·0098	0·0535	0·0535	0·125
3·84	0·976	0·0090	0·0555	0·054	0·114
4·85	0·993	—	0·056	—	—
5·38	0·992	0·0095	0·056	0·051	—
6·08	0·992	0·0095	0·0565	0·053	0·111
7·02	0·995	0·0098	0·057	0·0525	0·109
8·3	0·983	—	0·0565	—	—
8·8	0·970	0·0100	0·0555	0·0525	0·112
10·5	0·980	—	0·056	—	—
12·9	0·970	0·0096	0·056	0·054	0·105

$C_{D\,\min}$ occurs at $\alpha = 0{\cdot}7$ deg approx. and $C_L = 0{\cdot}01$ to $0{\cdot}02$.

Change of slope occurs at mean values of C_L of about $0{\cdot}35$ and of α about $6\frac{1}{2}$ deg but the scatter of the changeover points is considerable.

TABLE 5

Tufts			Balance Measurements		
			α (degrees) at		
$\frac{R}{10^6}$	α at instantaneous change in flow pattern (degrees)	$\frac{R}{10^6}$	Critical change in value of dC_m/dC_L	Minimum in C_m vs. α curve	Commencement of severe loss of lift
	A		B	C	D
—	—	0·515	5	$8\frac{3}{4}$	11
—	—	1·76	12	$13\frac{3}{4}$	14
3·3	17·0	—	—	—	—
4·2	18·8	3·84	$18\frac{3}{4}$		
—	—	4·85	$18\frac{1}{4}$	19	18·7
—	—	5·38	19	19·5	19·5
6·0	19·0	6·08	19	19·7	19·7
6·8	18·7	7·02	$19\frac{1}{4}$	19·3	19
7·8	18·4	—	—		
7·85	17·75 }	8·3	$18\frac{1}{4}$	19	18·5
,,	18·0 }	—			
8·8	17·75	8·8	—	19	18·6
9·6	17·5	—	—		
10·0	17·0	—	—		
10·9	17·0	10·5	17	18·6	18·5
11·5	16·2	—	—	—	—
12·8	16·6	12·9	$16\frac{1}{4}$	$17\frac{1}{4}$	$17\frac{1}{4}$
13·6	15·5 }	—	—	—	—
,,	16·0 }	—	—	—	—

Compare A with B, C with D.

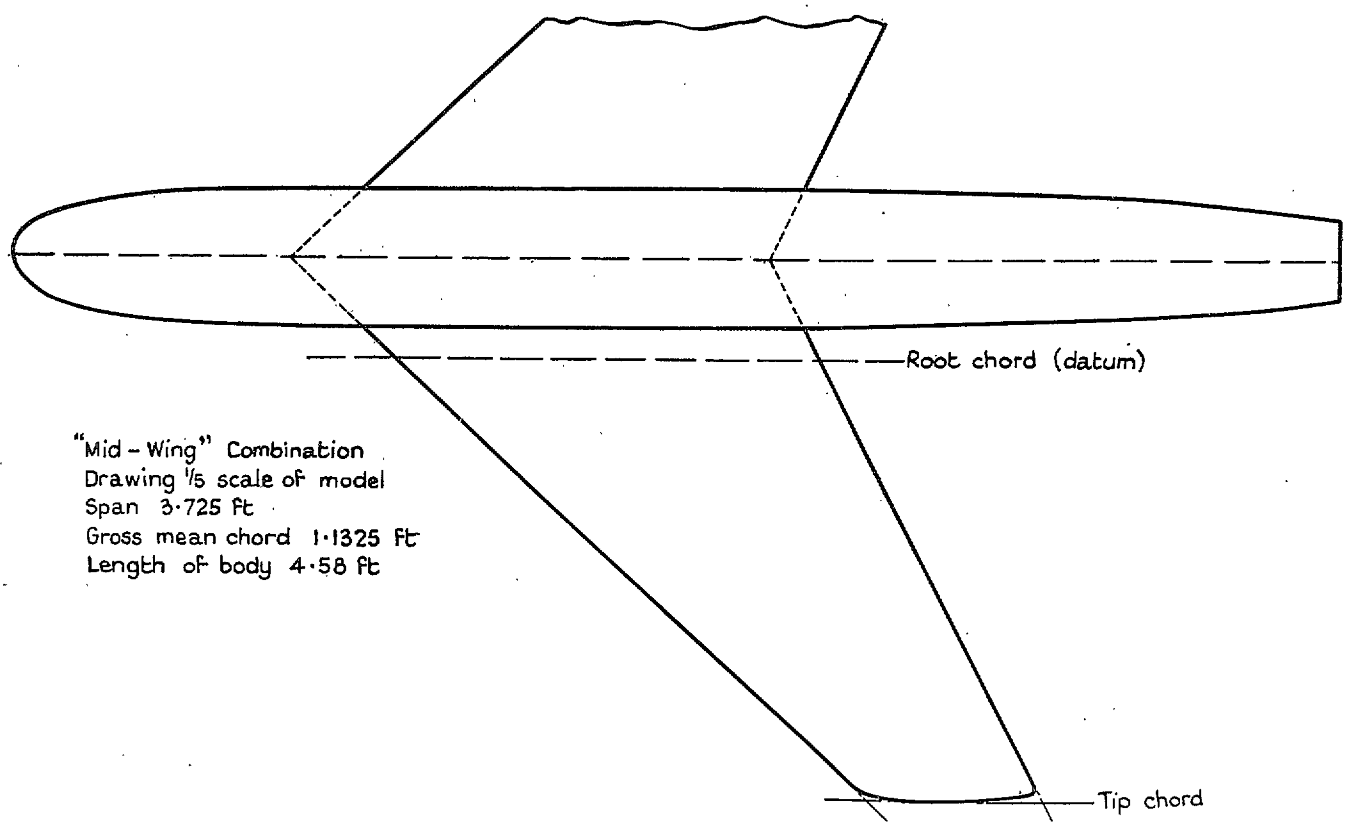

FIG. 1. Plan of model.

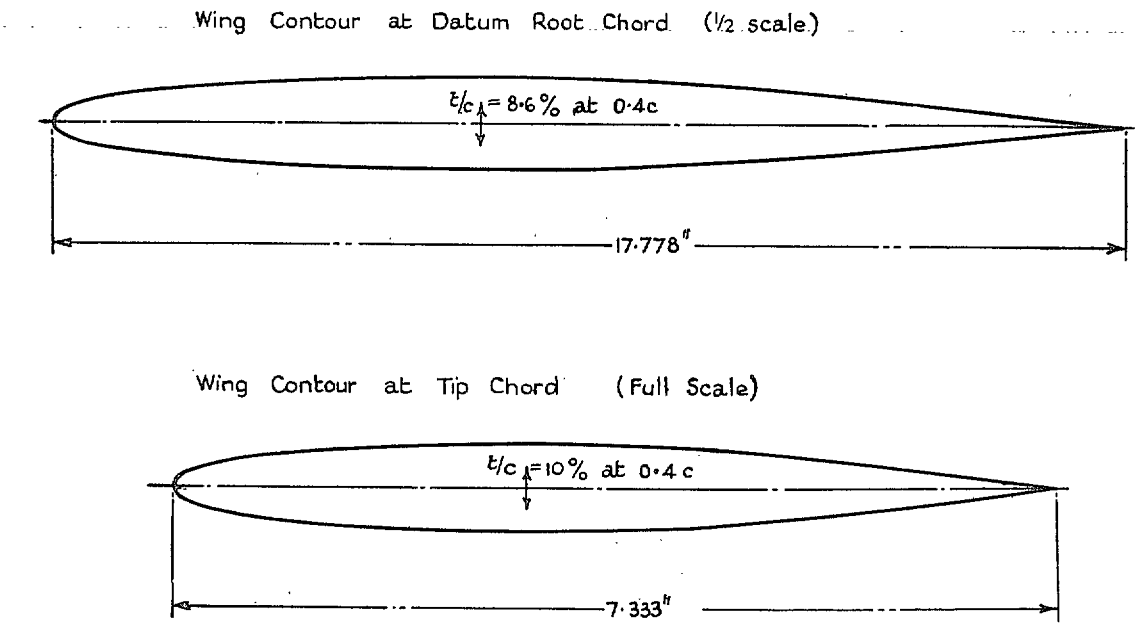

FIG. 2. Wing profiles.

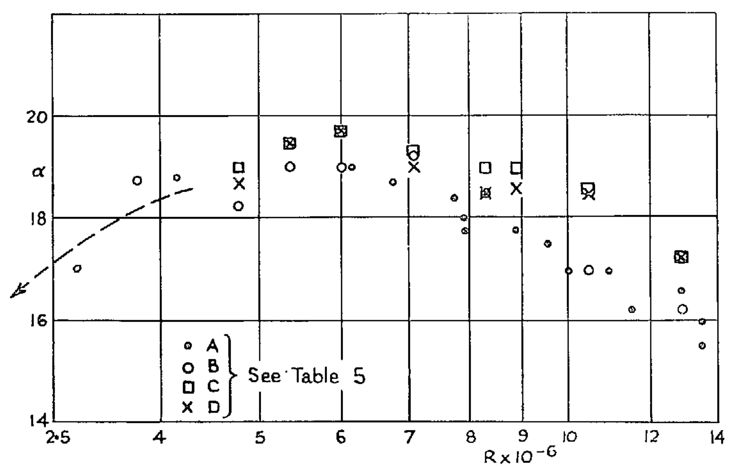

Critical $dC_m/d\alpha$ and flow pattern.

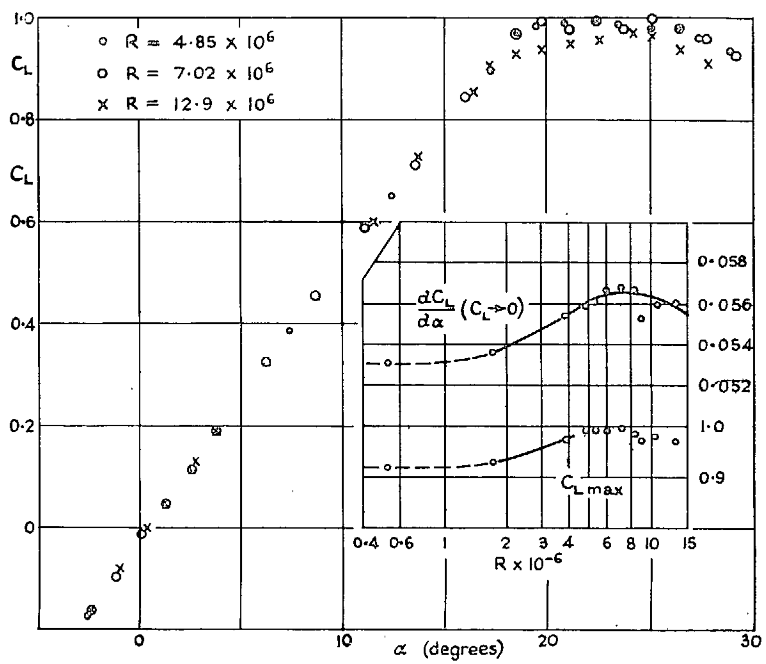

Lift coefficient and incidence.

FIG. 3.

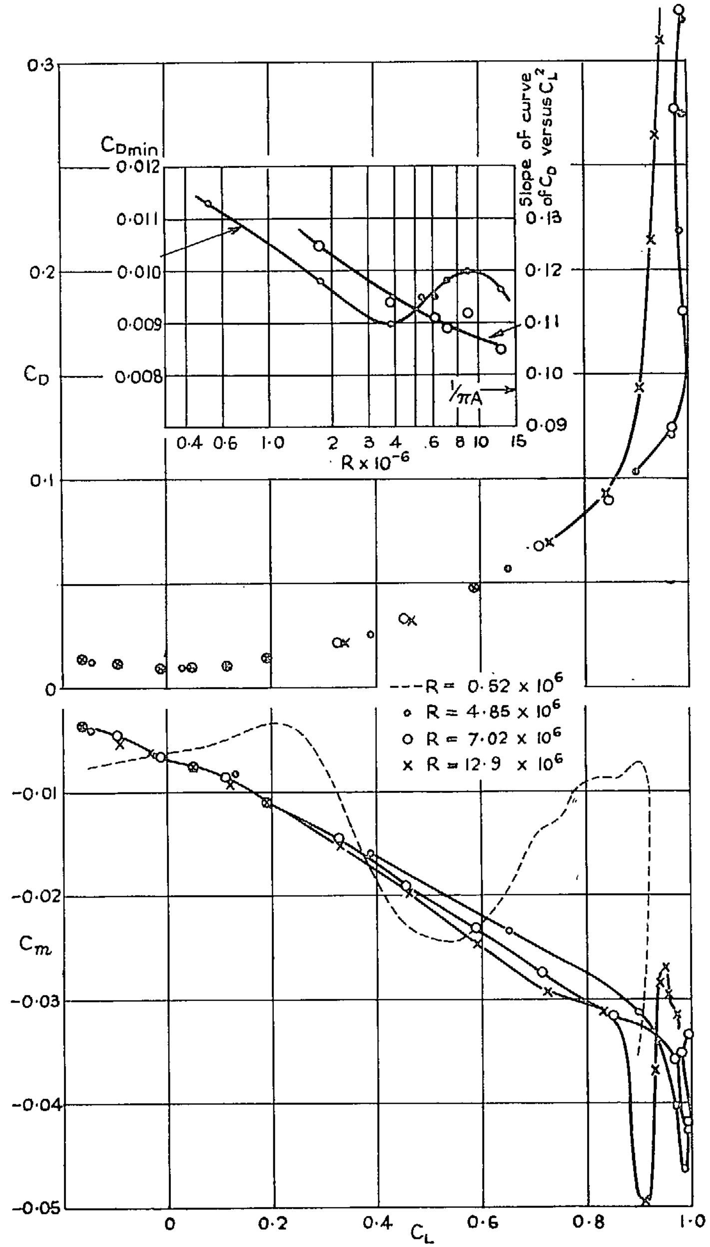

FIG. 4. Drag and pitching moment.

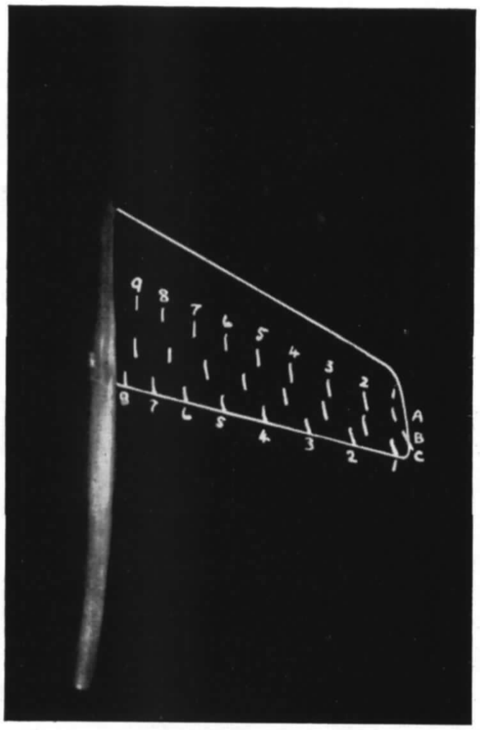

FIG. 5a.

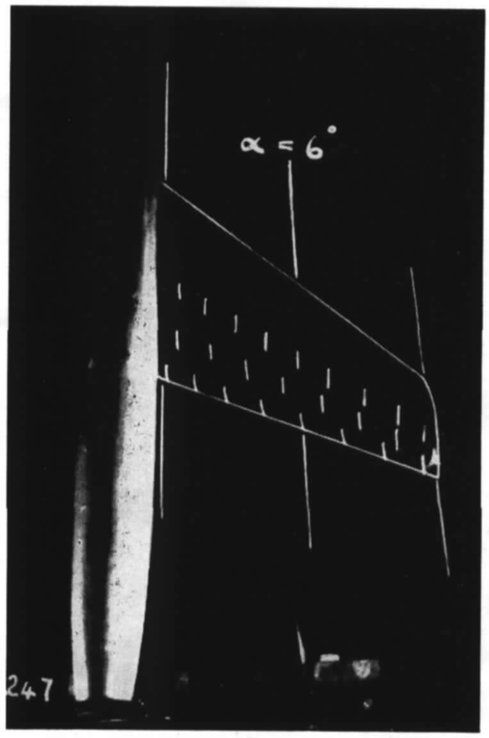

FIG. 5b.

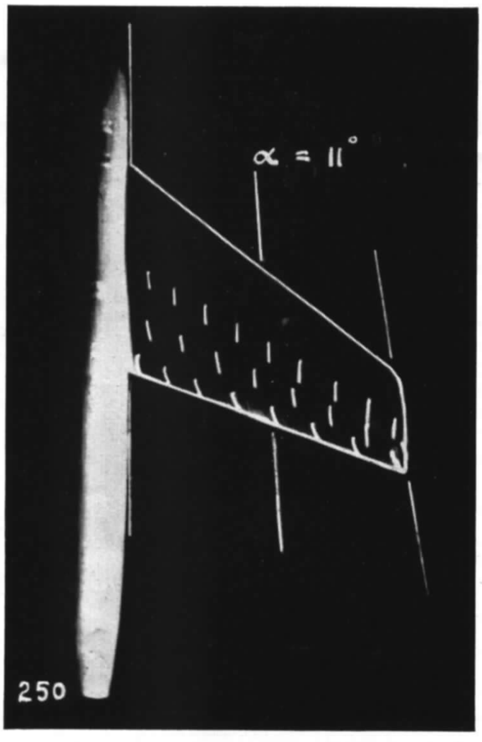

FIG. 5c.

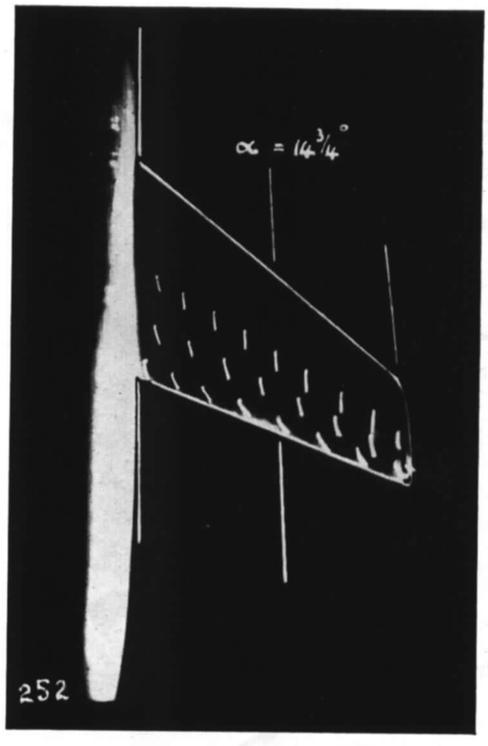

FIG. 5d.

Tuft photographs.

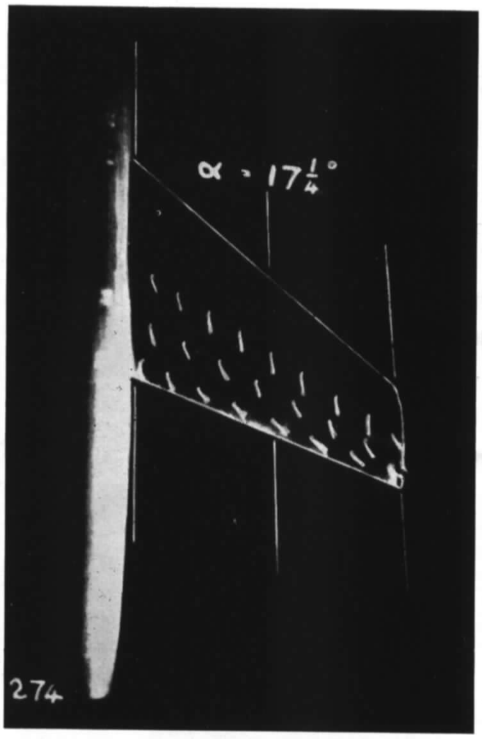

FIG. 6a.

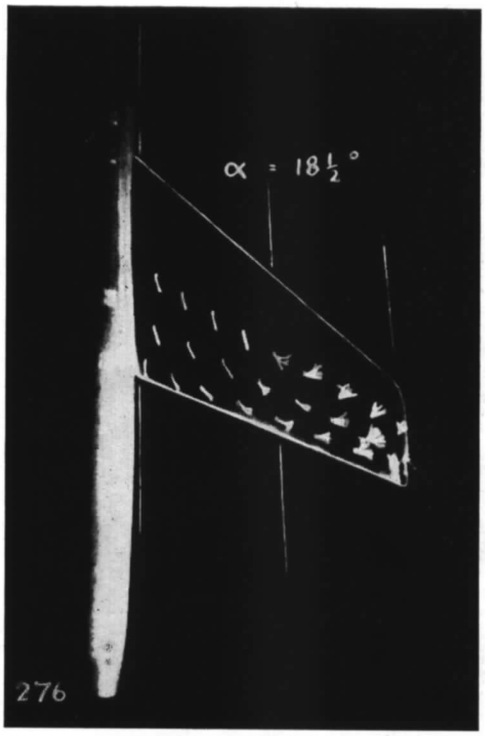

FIG. 6b.

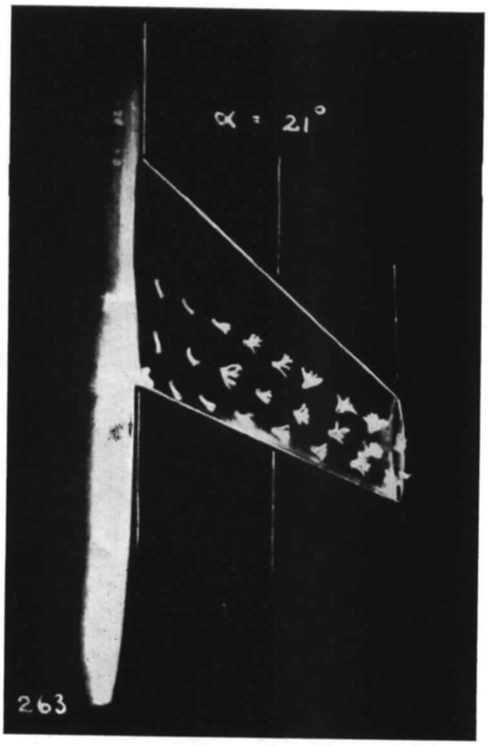

FIG. 6c.

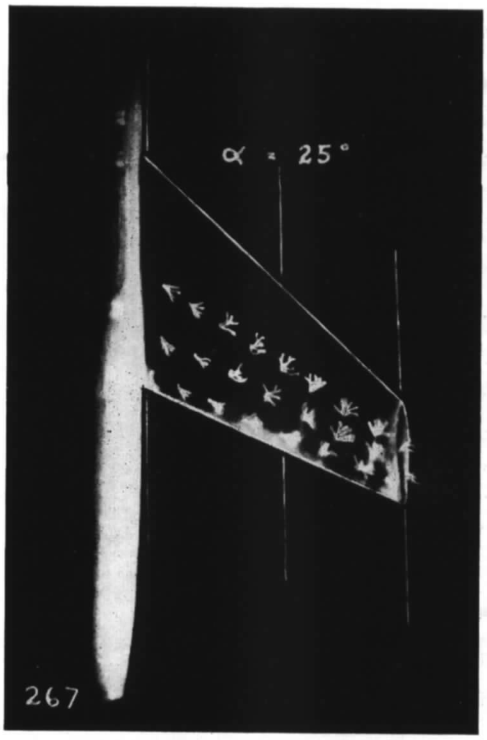

FIG. 6d.

Tuft photographs.

(23118) Wt. 15-680 K9 10/53 F. M. & S.

PRINTED IN GREAT BRITAIN

R. & M. No. 2738
(13,155)
A.R.C. Technical Report

Publications of the Aeronautical Research Council

ANNUAL TECHNICAL REPORTS OF THE AERONAUTICAL RESEARCH COUNCIL (BOUND VOLUMES)

1936 Vol. I. Aerodynamics General, Performance, Airscrews, Flutter and Spinning. 40*s.* (40*s.* 9*d.*)
Vol. II. Stability and Control, Structures, Seaplanes, Engines, etc. 50*s.* (50*s.* 10*d.*)

1937 Vol. I. Aerodynamics General, Performance, Airscrews, Flutter and Spinning. 40*s.* (40*s.* 10*d.*)
Vol. II. Stability and Control, Structures, Seaplanes, Engines, etc. 60*s.* (61*s.*)

1938 Vol. I. Aerodynamics General, Performance, Airscrews. 50*s.* (51*s.*)
Vol. II. Stability and Control, Flutter, Structures, Seaplanes, Wind Tunnels, Materials. 30*s.* (30*s.* 9*d.*)

1939 Vol. I. Aerodynamics General, Performance, Airscrews, Engines. 50*s.* (50*s.* 11*d.*)
Vol. II. Stability and Control, Flutter and Vibration, Instruments, Structures, Seaplanes, etc. 63*s.* (64*s.* 2*d.*)

1940 Aero and Hydrodynamics, Aerofoils, Airscrews, Engines, Flutter, Icing, Stability and Control, Structures, and a miscellaneous section. 50*s.* (51*s.*)

1941 Aero and Hydrodynamics, Aerofoils, Airscrews, Engines, Flutter, Stability and Control, Structures. 63*s.* (64*s.* 2*d.*)

1942 Vol. I. Aero and Hydrodynamics, Aerofoils, Airscrews, Engines. 75*s.* (76*s.* 3*d.*)
Vol. II. Noise, Parachutes, Stability and Control, Structures, Vibration, Wind Tunnels. 47*s.* 6*d.* (48*s.* 5*d.*)

1943 Vol. I. (In the press.)
Vol. II. (In the press.)

ANNUAL REPORTS OF THE AERONAUTICAL RESEARCH COUNCIL—

1933-34	1*s.* 6*d.* (1*s.* 8*d.*)	1937	2*s.* (2*s.* 2*d.*)
1934-35	1*s.* 6*d.* (1*s.* 8*d.*)	1938	1*s.* 6*d.* (1*s.* 8*d.*)
April 1, 1935 to Dec. 31, 1936.	4*s.* (4*s.* 4*d.*)	1939-48	3*s.* (3*s.* 2*d.*)

INDEX TO ALL REPORTS AND MEMORANDA PUBLISHED IN THE ANNUAL TECHNICAL REPORTS AND SEPARATELY—
April, 1950 - - - - - R. & M. No. 2600. 2*s.* 6*d.* (2*s.* 7½*d.*)

AUTHOR INDEX TO ALL REPORTS AND MEMORANDA OF THE AERONAUTICAL RESEARCH COUNCIL—
1909-1949 - - - - - R. & M. No. 2570. 15*s.* (15*s.* 3*d.*)

INDEXES TO THE TECHNICAL REPORTS OF THE AERONAUTICAL RESEARCH COUNCIL—

December 1, 1936—June 30, 1939.	R. & M. No. 1850.	1*s.* 3*d.* (1*s.* 4½*d.*)
July 1, 1939—June 30, 1945.	R. & M. No. 1950.	1*s.* (1*s.* 1½*d.*)
July 1, 1945—June 30, 1946.	R. & M. No. 2050.	1*s.* (1*s.* 1½*d.*)
July 1, 1946—December 31, 1946.	R. & M. No. 2150.	1*s.* 3*d.* (1*s.* 4½*d.*)
January 1, 1947—June 30, 1947.	R. & M. No. 2250.	1*s.* 3*d.* (1*s.* 4½*d.*)
July, 1951. - - - - -	R. & M. No. 2350.	1*s.* 9*d.* (1*s.* 10½*d.*)

Prices in brackets include postage.

Obtainable from

HER MAJESTY'S STATIONERY OFFICE

York House, Kingsway, London, W.C.2; 423 Oxford Street, London, W.1 (Post Orders: P.O. Box 569, London, S.E.1); 13a Castle Street, Edinburgh 2; 39 King Street, Manchester 2; 2 Edmund Street, Birmingham 3; 1 St. Andrew's Crescent, Cardiff; Tower Lane, Bristol 1; 80 Chichester Street, Belfast or through any bookseller.

S.O. Code No. 23-2738